# Invertebrate methylomes provide insight into mechanisms of environmental tolerance and reveal methodological biases

Shelly A. Trigg*[1], Yaamini R. Venkataraman*[1], Mackenzie R. Gavery[2], Steven B. Roberts[1], Debashish Bhattacharya[3], Alan Downey-Wall[4], Jose M. Eirin-Lopez[5], Kevin M. Johnson[6,7], Katie E. Lotterhos[4], Jonathan B. Puritz[8] and Hollie M. Putnam[8+]

[1] University of Washington, School of Aquatic and Fishery Sciences 1122 NE Boat St. Seattle, WA, 98195, USA
[2] Environmental and Fisheries Sciences Division, Northwest Fisheries Science Center, National Marine Fisheries Service, National Oceanic and Atmospheric Administration, 2725 Montlake Blvd E, Seattle, WA, 98112, USA
[3] Department of Biochemistry and Microbiology, Rutgers University, New Brunswick, NJ 08901 USA
[4] Department of Marine and Environmental Sciences, Northeastern University, 430 Nahant Road, Nahant, MA 01908
[5] Florida International University, Environmental Epigenetics Laboratory, Institute of Environment 3000 NE 151 St. North Miami, FL, 33181, USA
[6] Center for Coastal Marine Sciences, California Polytechnic State University, San Luis Obispo, CA, 93407, USA
[7] California Sea Grant, University of California San Diego, La Jolla, CA, 92093
[8] Department of Biological Sciences, University of Rhode Island, Kingston, RI 02881, USA

[+] corresponding author: hputnam@uri.edu

* joint first authors/equal contribution

Keywords: bisulfite sequencing, coral, epigenetics, marine invertebrate

## Abstract

There is a growing focus on the role of DNA methylation in the ability of marine invertebrates to rapidly respond to changing environmental factors and anthropogenic impacts. However, genome-wide DNA methylation studies in non-model organisms are currently hampered by limited understanding of methodological biases. Here we compare three methods for quantifying DNA methylation at single base pair resolution — Whole Genome Bisulfite Sequencing (WGBS), Reduced Representation Bisulfite Sequencing (RRBS), and Methyl-CpG Binding Domain Bisulfite Sequencing (MBDBS) — using multiple individuals from two reef-building coral species with contrasting environmental sensitivity. All methods reveal substantially greater methylation in *Montipora capitata* (11.4%) than the more sensitive *Pocillopora acuta* (2.9%). The majority of CpG methylation in both species occurs in gene bodies and flanking regions. In both species, MBDBS has the greatest capacity for detecting CpGs in coding regions at our sequencing depth, however MBDBS may be limited by intra-sample methylation heterogeneity. RRBS yields robust information for specific loci albeit without enrichment of any particular genome feature and with significantly reduced genome coverage. Relative genome size strongly influences the number and location of CpGs detected by each method when sequencing depth is limited, illuminating nuances in cross-species comparisons. These findings reinforce the role and importance of DNA methylation underlying environmental sensitivity in critical marine invertebrate taxa, and provide a genomic resource for investigating the functional role of DNA methylation in environmental tolerance.

## Introduction

Environmental stimuli interact with genomic content to drive variation in gene and protein expression, resulting in phenotypic plasticity. This plasticity has the potential to buffer against mortality under environmental change (Baldwin, 1902), or conversely be maladaptive (Velotta et al., 2018). Furthermore, plasticity may enhance or diminish evolutionary rates (Ghalambor et al., 2007), which is particularly relevant to plasticity-evolution feedbacks (Ghalambor et al., 2007, 2015; Kronholm & Collins, 2016). This is of particular concern in the Anthropocene (Lewis & Maslin, 2015), as global change exacerbates the mismatch between phenotype and a rapidly changing environment.

The increase in negative global climate change consequences have prompted an intensification of research into phenotypic plasticity, gene regulation, and epigenetic mechanisms in non-model marine invertebrates (Eirin-Lopez & Putnam, 2019; Hofmann, 2017; Roberts & Gavery, 2012). Specifically, carryover effects and cross and multi-generational plasticity in response to climate change (Byrne et al., 2020) may be generated by epigenetic regulation of gene expression (Dixon et al., 2018; Liew et al., 2018, 2020). As epigenetic research has increased, there has been a focus on DNA methylation, or the addition of a methyl group on the Cytosine residues in the genome, often in the Cytosine phosphate Guanine, or CpG context (Zemach et al., 2010). DNA methylation has gene expression regulation capacity through the interaction of base modification with transcriptional elements. Early bulk enzyme-based and fingerprinting methods for quantifying DNA methylation in marine invertebrates provided initial insights into DNA methylation and organismal phenotypic plasticity in response to environmental

changes (Dimond et al., 2017; Gavery & Roberts, 2010; Gonzalez-Romero et al., 2017; Putnam et al., 2016; Rodriguez-Casariego et al., 2018; Suarez-Ulloa et al., 2018).

Non-sequencing approaches that quantify global or bulk methylation [e.g., colorimetric or fluorescent ELISAs (Dimond et al., 2017; Gavery & Roberts, 2010; Putnam et al., 2016; Rodriguez-Casariego et al., 2018)] are low-cost, rapidly applied, and do not require genomic resources to generate information on the responsiveness of the methylome. These global estimates do not, however, fully capture local changes in DNA methylation across different genome regions. Specifically, differences in the location and amount of methylation in two samples or treatments could lead to an incorrect conclusion when based on average percent methylation at the bulk level. Consequently, non-sequencing methods are limited in their ability to elucidate specific mechanisms of expression regulation and thus are unable to fully address the functional implications of methylation-driven regulation within the genome. In contrast, the use of genome-wide approaches that provide single base pair resolution allow the testing of hypotheses regarding spurious transcription, alternative splicing, and exon skipping (Roberts & Gavery, 2012). For example, the use of Whole Genome Bisulfite Sequencing (WGBS) to investigate the role of DNA methylation in regulating genes involved in caste specification in honeybees identified differential methylation in an exon of the *anaplastic lymphoma kinase (ALK)* gene; this exon was differentially retained in a splice variant between queens and workers (Foret et al., 2012). Thus there is a clear need for single base pair assessment of DNA methylomes facilitated by next generation sequencing to more fully elucidate the relationship of DNA methylation and gene expression in non-model invertebrates.

Genome-wide levels of DNA methylation can be estimated by several bisulfite conversion and sequencing approaches. Bisulfite conversion of DNA results in the deamination of unmethylated Cytosine to Uracil, which leaves a base change signature in the DNA that can be tracked via comparison of sequence between bisulfite-converted samples and reference genomes. While the number of bisulfite sequencing approaches are expanding [e.g., epiGBS (van Gurp et al., 2016)], the widely-used approaches are WGBS, Reduced Representation Bisulfite Sequencing (RRBS), and more recently, Methyl-CpG Binding Domain Bisulfite Sequencing (MBDBS). WGBS is considered to be the gold-standard of bisulfite sequencing because it provides full coverage of the genome and the capacity to detect the entire methylome at single base pair resolution.

While providing a comprehensive approach, the high cost of WGBS is juxtaposed against the often very small fraction of methylated DNA common in invertebrate genomes (Tweedie et al., 1997). Alternatively, approaches such as RRBS also use bisulfite conversion to quantitatively assess DNA methylation with base pair resolution. RRBS incorporates a restriction digestion of the genome to enrich for CpG rich regions, and is designed to capture the majority of promoters and other genomic regions containing CpG islands because they have important regulatory functions in vertebrates (Meissner et al., 2008). This is a more cost-effective approach provided by sequencing only a small portion of the genome, but requires restriction enzyme recognition sites near other CpGs to gather high resolution data.Since DNA methylation in invertebrates is primarily limited to coding regions (Dixon et al., 2018; Flores et al., 2012; Roberts & Gavery, 2012), it is less clear whether enrichment of CG-rich DNA using RRBS will capture informative or regulatory

regions of invertebrate genomes, making the cost savings moot in the absence of informative data.

In contrast to the CpG-rich, region-specific targeting of RRBS, MBDBS uses Methyl Binding Domain Proteins to target and enrich methylated CpGs, then employs bisulfite conversion to provide single base pair resolution of DNA fragments with methylated regions. Many marine invertebrate genomes consist of highly methylated regions that are distributed in predominantly unmethylated DNA in a mosaic pattern (Suzuki et al., 2007). When invertebrate methylomes have been characterized, these highly methylated regions overlap with gene bodies and have been shown to play a role in gene expression activity (Roberts & Gavery, 2012). Therefore, using an enrichment approach such as MBDBS to isolate gene body methylation can be a cost-effective and gene-body focused alternative to WGBS or RRBS (Gavery & Roberts, 2013; Venkataraman et al., 2020). The base-pair resolution offered by the combination of MBD enrichment and BS is an advantage compared to MBD-seq alone (Dixon & Matz, 2020), as the latter assumes that methylation level is proportional to read depth. In contrast to WGBS or RRBS, the quantification and interpretation of MBDBS data can be complicated by individual variation in methylation levels (e.g., one individual who has high methylation in a particular region would have reads, whereas another individual who lacks methylation in that region would have missing data).

Given the need to assess plasticity mechanisms and the acclimatization potential of a variety of marine taxa, it is critical to compare the potential of different approaches to to detect, quantify, and assess DNA methylation with respect to specific biological hypotheses of interest. To this end, we studied three DNA methylation quantification

approaches that provide single base pair resolution data using bisulfite conversion and sequencing: WGBS, RRBS, and MBDBS. We applied these methods to two reef building corals, *Montipora capitata* and *Pocillopora acuta*, which have different environmental sensitivity, phenotypic plasticity, inducible DNA methylation (Putnam et al., 2016), and genome sizes (Shumaker et al., 2019; Vidal-Dupiol et al., 2019). We assessed species-specific differences in genome-wide methylation and contrasted percent methylation of common loci and orthologous genes across methods. Then, we compared the coverage and genomic location of CpG data generated from the three methods. Compared to WGBS, both MBDBS and RRBS have advantages and potential limitations associated with biology, genome characteristics, and experimental design, highlighting the need to fully consider these aspects when evaluating DNA methylation for particular hypotheses of function in invertebrates. As part of this effort, we described DNA methylation differences in two coral species, providing valuable insights into the epigenetic underpinnings of phenotypic plasticity.

## Materials and Methods

### *Sample collection*

The reef-building scleractinian coral species *Montipora capitata* and *Pocillopora acuta* were collected from the reefs of Kane‘ohe Bay Hawai‘i under SAP 2019-60 between 4 - 7 September 2018. Corals were transported to the Hawai‘i Institute of Marine Biology where they were held in tanks under ambient conditions for 15 days and then snap frozen in liquid nitrogen and stored at -80°C until nucleic acid extraction was performed. For each

of the two coral species, fragments were collected from three different individuals collected from ambient conditions.

*Nucleic Acid Extraction*

Samples were removed from -80°C and small tissue fragments were clipped directly into a tube containing RNA/DNA shield (1 ml) and glass beads (0.5 mm). The tissue clippings consisted of all coral cell types and their symbionts. Samples were homogenized on a vortexer for 1 minute for the thin tissue imperforate coral *Pocillopora acuta* and 2 minutes for the thick tissue perforate coral *Montipora capitata* at maximum speed to ensure tissue extraction of all cell types. The supernatant was removed and DNA was extracted using the Zymo Quick-DNA/RNA™ Miniprep Plus Kit and subsequently checked for quality using gel electrophoresis on an Agilent 4200 TapeStation and quantified using a Qubit. In summary, one DNA preparation was made from each of the three individuals per coral species and was subsequently divided into three aliquots for each of the three bisulfite sequencing methods (WGBS, MBDBS, and RRBS) to yield a total of 18 libraries (**Figure 1**).

*Genome Information*

Previously sequenced and assembled coral genomes were used for mapping of DNA methylation data. These include *Montipora capitata* (Shumaker et al., 2019) and *Pocillopora acuta* (Vidal-Dupiol et al., 2019). Both of the coral genomes have a high and similar number of predicted genes (63,227 in *M.capitata* and 64,558 in *P. acuta*). However, *P. acuta* is much smaller in size (~352MB vs. ~886 MB in *M. capitata*), has less repetition,

a greater number of scaffolds (25,553 in *P. acuta* vs. 3,043 in *M.capitata*), and lower genome assembly continuity (N50 is 171,375 in *P. acuta* and 540,623 in *M. capitata*).

Genome feature tracks for *M. capitata* and *P. acuta* were derived directly from the published genomes for use in DNA methylation analyses. The *M. capitata* genome annotation yielded gene (a combination of AUGUSTUS and GeMoMa predictions), coding sequence, and intron tracks (Shumaker et al., 2019). Similarly, gene (AUGUSTUS predictions), coding sequence, and intron information was obtained from the *P. acuta* genome (Vidal-Dupiol et al., 2019). Flanking regions upstream and downstream of genes were generated with BEDtools v2.29.2 for each genome separately (Quinlan & Hall, 2010); `flankBED` was used to generate 1000 bp flanks upstream and downstream of annotated genes from each genome. Overlaps between genes and flanks were removed from up- or down-stream flanking region tracks using `subtractBED`. Similarly, an intergenic region track was created by finding the complement of genes with `complementBED`, then removing any overlaps with flanking regions using `subtractBED`. All tracks were verified with the Integrative Genomics Viewer (Thorvaldsdóttir et al., 2013). Feature track files generated for both species are available in the project large file repository (Putnam et al., 2020)

*MBD Enrichment*

Before enrichment, DNA (1 µg) in 80 µL Tris HCl was sheared to 500 bp using a QSonica Q800R3. Samples were sonicated for 90 sec, with 15 sec on and 15 sec off intervals at 25% amplitude. Fragment length was checked using a D5000 TapeStation

System (Agilent Technologies) and samples were sonicated an extra 15 sec to shear DNA from 600 bp to 500 bp as needed.

The MethylMiner kit (Invitrogen; Cat. #ME10025) was used to enrich for methylated DNA prior to MBDBS library generation, with 1µg of input DNA. Manufacturer's instructions were adhered to with the following modifications: The capture reaction containing the fragmented DNA and MBD beads was incubated with mixing at 4ºC overnight, and enriched DNA was obtained with a single fraction elution using 2,000 mM NaCl. Following ethanol addition, samples were centrifuged at 14,000 rcf at 1ºC for five min. Pellets were resuspended in 25 µL ultra-pure water. Captured DNA was quantified using a Qubit dsDNA HS Kit (Invitrogen).

*MBDBS and WGBS Library Preparation*

WGBS and MBDBS libraries were prepared using the Pico Methyl-Seq Library Prep Kit (ZymoResearch Cat. # D5456). Manufacturer's instructions were followed with the following modifications: For each sample, 1 ng of coral DNA and 0.05 ng of lambda phage DNA (ZymoResearch Cat. # D5016) were used. Samples were always centrifuged at 12,000 rcf for 30 sec, however, samples were centrifuged for 12,000 rcf for 90 sec after the second 200 µL addition of M Wash Buffer. Warmed elution buffer (56°C) was added to each sample to increase DNA elution yield. During the second amplification cycle, 0.5 µL of PreAmp Polymerase was added. After initial clean-up with the DNA Clean-up and Concentrator, the first amplification step was run for eight cycles. For amplification with i5 and i7 index primers, 1 µL of each primer was used to improve amplification. The volume

of the 2X LibraryAmp Master Mix was increased to 14 µL to match the increase in index primers.

To remove excess primers from WGBS and MBDBS preparations, samples were cleaned with 11 µL of KAPA pure beads (1X) (KAPA Cat # KK8000) and 80% ethanol. Cleaned samples were resuspended in 12 µL of room-temperature DNA elution buffer from the Pico Methyl-Seq Library Prep Kit. Samples were re-amplified with either two or four cycles, depending on DNA concentration. Re-amplification was conducted with only 0.5 µL of each i5 and i7 index primer. After re-amplification, 26 µL of KAPA pure beads (1X) and 80% ethanol were used for clean-up. Final samples were resuspended in 14 µL of room-temperature elution buffer. Primer removal was confirmed by running samples on a D5000 TapeStation System.

*RRBS Library Prep*

RRBS libraries were prepared with the EZ DNA RRBS Library Prep Kit (ZymoResearch Cat. # D5460). Manufacturer's instructions were used with the following modifications: For MspI digestion, 300 ng of input DNA and 15 ng of lambda phage DNA were used. Digestions were carried out at 37°C for 4 hours. Adapter ligation was performed overnight, with samples held at 4°C once cycling was completed. Similar to WGBS and MBDBS library preparation, samples were always centrifuged at 12,000 rcf for 30 sec, with the exception of 90 sec centrifugation after the second 200 µL addition of M Wash Buffer. Warmed elution buffer (56°C) was added to each sample to increase DNA elution yield. Index primers were ligated using eleven cycles of the recommended thermocycling protocol. Samples were cleaned using 50 µL of KAPA pure beads (1X) and

80% ethanol, then resuspended in 16 µL of the elution buffer. Primer removal was confirmed by running samples on a D5000 TapeStation System.

*DNA Sequence Alignment*

All libraries (n = 18) were pooled in equimolar amounts and loaded at 250 pM onto a single Illumina NovaSeq S4 flow cell lane for 2x150 bp sequencing at Genewiz (South Plainfield, NJ). This was estimated to give 111-138 M reads per library and 99-123x coverage of the *P. acuta* genome (3.3 M bp) and 38-47x coverage of the *M. capitata* genome (8.8 M bp), assuming 100% even coverage (e.g., 150 bp read * 2 pairs * 111 M reads/336,684,533 bp for *P. acuta*).

Sequence quality was checked by FastQC v0.11.8 and adapters from paired-end sequences were trimmed using TrimGalore! version 0.4.5 (Krueger, 2012). Following recommendations for methylation sequence analysis from the manufacturer's protocol and from the Bismark User Guide, 10 bp were hard trimmed from the 5' and 3' end of each read for WGBS and MBDBS samples, and RRBS samples were trimmed with `--non_directional` and `--rrbs` options. Bisulfite-converted genomes were created in-silico with Bowtie 2-2.3.4 [Linux x84_64 version; (Langmead & Salzberg, 2012)) using `bismark_genome_preparation` through Bismark v0.21.0 (Krueger & Andrews, 2011). Trimmed reads were aligned to the BS-converted *P. acuta* genome (Vidal-Dupiol et al., 2019) and the BS-converted *M. capitata* genome (Shumaker et al., 2019) with Bismark v0.21.0 with alignment stringency set by `-score_min L,0,-0.6` and the default MAPQ score threshold of 20. To check mapping rates for endosymbionts and quantify percent

methylation, trimmed reads from *P. actua* libraries were also aligned to the *Cladicopium goreaui* genome [type C1, previously *Symbiodinium goreaui* (Liu et al., 2018)] using the same settings as specified above. Reads that mapped ambiguously were excluded and alignment files containing uniquely mapped reads were deduplicated with `deduplicate_bismark` for WGBS and MBDBS samples only. Methylation calls were extracted from sorted deduplicated alignment files using `bismark_methylation_extractor`. Cytosine coverage reports were generated using `coverage2cytosine` with the `--merge_CpG` option to combine data from both strand methylation. Resulting files include bedgraphs and Bismark coverage files (Putnam et al., 2020). MultiQC v1.8 (Ewels et al., 2016) was run on the trimmed reads, FastQC output, and Bismark reports to assess quality and summarize results.

*Bisulfite conversion efficiency assessment*

Trimmed sequence reads were aligned to the genome of *E. coli* strain K-12 MG1655 (Riley et al., 2006) using Bismark v0.21.0 with the `-non_directional` option and alignment stringency set by `-score_min L,0,-0.6`. Bisulfite conversion efficiency was also estimated from coral alignments as the ratio of the sum of unmethylated cytosines in CHG and CHH context to the sum of methylated and unmethylated cytosines in CHG and CHH. ANOVA was used to test for an effect of library preparation method on conversion efficiency within each species (conversion efficiency ~ library preparation method) for both estimated and lambda alignment calculated conversion efficiencies. A two-sample t-test was used to test if conversion

efficiency calculated from lambda alignments was the same as estimated conversion efficiency for each library preparation method within each species.

*Genome-Wide Methylation*

General *M. capitata* and *P. acuta* methylation was characterized to describe any species specific patterns. This was carried out by combining BEDgraphs derived from all methods for each species using `unionBedGraphs`. Percent methylation for every CpG locus with at least 5x coverage was averaged, irrespective of how many samples had coverage for that locus. Loci with no data within a method were excluded from downstream analysis. CpGs were classified as being either highly methylated (≥ 50% methylation), moderately methylated (>10% and <50%), or lowly methylated (≤10% methylation).

*Percent Methylation of Shared CpG Loci*

Comparisons of percent DNA methylation at CpG loci analyzed by more than one method were performed using the R-package `methylKit` (Akalin et al., 2012). A minimum of 5x coverage was required across all samples for a CpG locus to be considered in the analyses. The `unite` function in methylKit was used to identify CpG loci that were covered across all 9 samples (3 individuals per method) per species. Scatterplots and Pearson correlation coefficients were calculated using the function `getCorrelation`. Additionally, differential methylation tests were performed on pairwise comparisons between methods (WGBS versus RRBS, WGBS versus MBDBS, and RRBS versus MBDBS). Discordant methylation was quantified using a logistic

regression model on CpG loci that were covered across all 6 samples (3 samples from each method compared) in each pairwise comparison using the `calculateDiffMeth` function with default parameters.

*CpG Coverage*

To assess average genome-wide CpG coverage, the number of Cytosines passing different read depth thresholds (5x, 10x, 15x, 20x, 25x, 30x, 40x, and 50x) were totaled from the CpG coverage reports output by the Bismark `coverage2cytosine` function (detailed above) for each sample. These totaled CpGs were then relativized to the number of CpGs in their respective genomes (*M. capitata,* 28,684,519 CpGs; *P. acuta,* 9,155,620 CpGs). Next, average and standard deviation of genome-wide CpG fractions were calculated for each method within each species (n = 3), and these were plotted across different read depth thresholds using ggplot2 (Gómez-Rubio, 2017).

To estimate overall genome-wide CpG coverage, a downsampling analysis was performed by pooling all sample reads within a method and species. Briefly, trimmed fastq files were concatenated for each method and species then randomly subsampled to 50, 100, 150, and 200 million reads. Next, alignment and methylation calling were carried out as described above on each subset, and the number of cytosines passing with 5 or more reads were totaled from CpG coverage reports from each subset. Sequencing saturation was estimated from a Michaelis-Menten model with the ‘drm’ function from the R package drc (Ritz et al., 2015) using CpG coverage reports from subsampled data as input. Both

observed CpG coverage from subsampled data and estimated CpG coverage were plotted using the R package ggplot2 (Gómez-Rubio, 2017).

*Proportion of Detected CpGs for Orthologs*

To describe the differences in DNA methylation detected by each method at a more functional level, and given the connection of gene body methylation and gene expression in invertebrates (Roberts & Gavery, 2012) and corals specifically (Liew et al., 2018), the presence of CpG data within all genes was calculated for each species, by method. First, a CpG gff track was generated using EMBOSS (Rice et al., 2011) with the `fuzznuc` command searching for the pattern CG. For each sample, `intersectBED` was used to identify CpGs with 5x coverage that intersected with gene regions. This was also done for the reference genome CpG gff track. CpG counts per gene were compiled for each sample and the mean taken per method. The proportion of CpGs per orthologous gene was calculated by dividing the mean number of CpGs with 5x coverage from the three samples per method and dividing that by the number of CpG possible summed per gene from the reference genome CpG gff track. The proportion of CpG data in a gene was then visualized in heatmaps for all genes of *M. capitata* and *P. acuta*.

*Genomic Location of CpGs*

For both *M. capitata* and *P. acuta*, the overlap between genome feature tracks and species-specific CpG data at 5x coverage was characterized with BEDtools v2.29.2 to assess the presence CpGs in various regions by method (Quinlan & Hall, 2010). Since only gene, coding sequence, intron, flanking regions, and intergenic region tracks were

common between species, these were the tracks used in downstream analyses. A combination of PCoA, PERMANOVA and beta-dispersion tests, and chi-squared contingency tests were used to determine if the library preparation method influenced the proportion of CpGs detected in a specific genomic feature. A separate contingency test was used for each genomic feature.

## Results

To compare the performance of bisulfite sequencing methods in the reef-building scleractinian corals *Montipora capitata* and *Pocillopora acuta*, we isolated DNA and generated WGBS, RRBS, and MBDBS libraries for three individuals from each species to yield a total of 18 libraries (**Figure 1**).

Sequencing of all 18 libraries resulted in 1.82 x $10^9$ read pairs, of which 99.1% remained after QC and trimming (Additional file 1: **Table ST1**). Individual libraries were generally sequenced to the same depth (~7.5 x $10^7$ reads) across library preparation methods and species, with the exception of *P. acuta* RRBS libraries, which were sequenced 2-4-fold deeper. The average mapping efficiencies for all *P. acuta* and all *M. capitata* libraries were 45% and 39% read alignments, respectively (Additional file 2: **Table ST2**). In comparison to other methods, MBDBS libraries had a larger proportion of reads (73.1% ± 9.9%) that did not align to the coral genomes (Additional file 3: **Figure SF1**). To investigate this we aligned *P. acuta* libraries to a known symbiont *Cladocopium goreaui* genome (C1 (Liu et al., 2018)) for which the genome sequence was available at the time of analysis. We found a sizable proportion of the MBDBS reads mapped to the symbiont genome (23.6 ± 10.6%), while a much smaller proportion of RRBS and WGBS reads

mapped to the symbiont genome (5.04 ± 0.22% and 1.92 ± 0.3% respectively) (Additional file 4: **Table ST3**).

Bisulfite conversion efficiency calculated from alignments of the unmethylated lambda DNA spike-in ranged from 98.6 to 99.3% in *M. capitata* and from 98.3 to 99.1% in *P. acuta* (Additional file 5: **Table ST4**), and this differed by library preparation method for both *M. capitata* ($F_{df}$= X, $P$ = 1.676e$^{-05}$) and *P. acuta* ($F_{df}$= X, $P$ = 0.025) libraries. In general, conversion efficiency calculated from the lambda alignments did not differ from conversion efficiency estimates from CHG and CHH methylation (under the assumption that non-CpG methylation does not occur in corals, see also (Liew et al., 2018)) from coral alignments in *M. capitata* and *P. acuta*. (Additional file 6: **Figure SF2** and Additional file 7: **Table ST5**).

For each species, the general methylation landscape was characterized for CpG loci with 5x coverage identified in any method. The *M. capitata* genome was more methylated than *P. acuta* (**Figure 2**). Using a cutoff of ≥ 50% methylation to define methylated CpGs, of the 13,340,268 CpGs covered by the *M. capitata* data, 11.4% were methylated. In contrast, only 2.9% of the 7,326,297 CpGs in *P. acuta* were methylated. Both genomes were predominantly lowly methylated (≤ 10% methylated): 79.6% CpGs in *M. capitata* and 91.3% CpGs in *P. acuta* were lowly methylated. The remaining 9.0% of CpGs in *M. capitata* and 5.8% of CpGs in *P. acuta* were moderately methylated (10-50% methylation). The different methods captured varying proportions of highly, moderately, and lowly methylated CpGs (Additional file 8: **Figure SF3**).

For quantitative comparison of method performance, we reduced the dataset to loci covered at 5x read depth across all methods and samples for each species, referred to here as 'shared loci'. The number of shared loci was 4,666 CpG for *M. capitata* and 93,714 CpG for *P. acuta*. A PCA of CpG methylation for loci covered at 5x read depth showed that libraries tended to cluster in PC space by preparation method, rather than by individual (Additional file 9: **Figure SF4**). Variation in methylation levels of the shared loci across all *M. capitata* samples was lower within a method than between methods (Additional file 9: **Figure SF4A**). In contrast, for *P. acuta*, RRBS and WGBS methods showed similar methylation levels of shared loci but these were different from the methylation level of loci identified in MBDBS (Additional file 9: **Figure SF4B**). To further explore the variation in methylation observed by method, we directly correlated quantitative methylation calls for the shared loci (**Figure 3**). For *M. capitata*, correlations among biological replicates within a method were higher, whereas for *P. acuta*, correlations were lower and more variable. Correlations between pairs of methods for *M. capitata* ranged on average from 0.75-0.82, whereas correlations for *P. acuta* ranged from 0.40-0.64. For *M. capitata*, WGBS versus MBDBS had the highest correlation. For *P. acuta*, WGBS versus RRBS had the highest correlation.

Discordance in methylation quantification between methods was evaluated by identifying the number of CpG loci with large differences (>50%) in methylation for each species. WGBS versus RRBS showed the lowest discordance in both species (0.4% for *M. capitata* and 0.5% for *P. acuta*). The highest discordance in methylation was found in comparisons with MBDBS for *P. acuta*, with 11% and 15% of CpG sites being called at least 50% different for comparisons with WGBS and RRBS, respectively. In contrast, only

0.4% and 5% of common CpG sites were at least 50% difference between MBDBS versus WGBS and MBDBS versus RRBS, respectively, for *M. capitata*. A majority of the discordance was due to higher methylation calls in MBDBS compared to WGBS or RRBS (**Figure 3B**).

Consistent with what would be expected based on genome size, *P. acuta* libraries have higher genome-wide CpG coverage than *M. capitata* regardless of library preparation method (**Figure 4A-C**). For both species, WGBS and MBDBS libraries covered more CpGs than RRBS libraries, whereas RRBS libraries tended to show greater read depth for the CpGs that it did cover. In other words, at >20x read depth, RRBS libraries covered more CpGs than either WGBS or MBDBS (**Figure 4** insets). Modelling increased sequencing depth for RRBS or MBDBS libraries showed little impact on the fraction of genome-wide CpGs covered in *M. capitata*, while increasing sequencing depth from 50 M to 200 M for WGBS libraries in both species and for MBDBS in *P. acuta* showed a substantially larger fraction of CpGs covered (Additional file 10: **Figure SF5**).

In order to assess the potential for cross-species comparisons using an equivalent dataset we quantified CpG data available across one-to-one orthologous genes. For *M. capitata*, WGBS yielded the highest proportion of CpGs, followed by RRBS, and then MBDBS (Additional file 11: **Figure SF6A**). This differed in *P. acuta* with WGBS yielding the highest proportion of CpGs on average across orthologs, followed by MBDBS, and then RRBS (Additional file 11: **Figure SF6B**).

In order to compare locations of CpG data between genomic features for each species and method, all CpGs with 5x coverage were characterized based on genomic feature location (**Figure 5)**. Global PERMANOVA tests found significant differences

454 between library preparation methods for CpG coverage in various genome features for *M.*
455 *capitata* and *P. acuta* (Additional file 12: **Table ST6**). Although post-hoc pairwise
456 PERMANOVA tests did not reveal differences between sequencing methods, power for
457 these was probably low (due to low sample size). Pairwise chi-squared tests indicated
458 there are differences in CpG location for both species. In particular, CpGs in gene bodies
459 were significantly enriched over other genomic features with MBDBS (**Figure 5**; Additional
460 file 13: **Table ST7**). Visual inspection of PCoA also revealed the proportion of CpGs
461 captured in coding sequences (CDS) drove differences between MBDBS and the other
462 methods in both species (**Figure 5C-D**).
463
464 **Discussion**
465 We evaluated the performance of three approaches that use bisulfite-treated library
466 preparation to enable single base pair resolution quantification of DNA methylation in
467 corals. Our results demonstrate that the methylation landscape can vary significantly
468 across species, which is a critical consideration for both interpreting environmental
469 response capacity, and therefore for experimental design. We report significant
470 differences in DNA methylation in two coral species that may contribute to their differential
471 environmental sensitivity of these organisms (Gibbin et al., 2015; Putnam et al., 2016).
472 Whereas WGBS is the gold standard for studying methylation, it comes at a high cost.
473 MBDBS enriches for gene regions, which may be useful for taxa with gene body
474 methylation. On the other hand, RRBS provides greater coverage depth for a smaller
475 fraction of the genome, but lacks specificity for genomic features, or DNA methylation.
476 Taken together, our findings indicate biology, genome architecture, regions of interest,

and depth of coverage are critical considerations when choosing methods for high resolution quantification of DNA methylation profiles in invertebrates.

*M. capitata* has a relatively high environmental tolerance (Bahr et al., 2016; Gibbin et al., 2015; Putnam et al., 2016), which has previously been attributed to its symbiont composition (Cunning et al., 2016), genome characteristics (Shumaker et al., 2019), perforate tissue-skeletal architecture and tissue thickness, and heterotrophic capacity (Rodrigues & Grottoli, 2007). Of particular relevance to DNA methylation are genomic aspects such as gene family duplication and high repeat content in *M. capitata* (Shumaker et al., 2019). Given genetic-epigenetic correlations, particularly in the case of DNA methylation and the requirement for a CpG sequence target site (Dimond & Roberts, 2020; Johnson et al., 2020), variation in genome architecture, gene number, and content will impact the presence and use of DNA methylation as a mechanism of gene expression regulation. We found overall DNA methylation was higher in *M. capitata* than in *P. acuta*, supporting early bulk analyses of DNA methylation in these species (Putnam et al., 2016). While the predicted number of genes is similar, the genome size of *M. capitata* is over twice that of *P. acuta* (Shumaker et al., 2019; Vidal-Dupiol et al., 2019). One explanation for the higher methylation in *M. capitata* is that with greater energy availability — through translocation from high density Symbiodiniaceae populations and energy stores in perforate tissues — there is greater capacity for maintenance methyltransferase to maintain high methylation, and thus reduce gene expression variability and spurious expression (Liew et al., 2018; Li et al., 2018). High constitutive methylation could allow "frontloading" of stress response genes (e.g., (Barshis et al., 2013)), providing greater stress tolerance. Another possible explanation is that the higher level of methylation

contributes to the silencing of repeated genetic elements. In contrast, with a small and non-repetitive genome, imperforate thin tissues, and low energy reserves, *P. acuta* may be more energetically limited. Thus, *P. acuta* may be expected to show lower DNA methylation across the genome as we demonstrate here, as well as a higher propensity for inducible methylation in the presence of stressors (Putnam et al., 2016).

Another striking contrast in DNA methylation in these species is the lack of concordance in the percent methylation values for *P. acuta* among methods compared to *M. capitata* (**Figure 3**). The potential for chimerism in corals (Oury et al., 2020; Schweinsberg et al., 2015) and differences in tissue structure (e.g., perforate or imperforate) between species could contribute to differences in concordance across methods for quantifying DNA methylation. One possibility is that Pocilloporids are chimeric and multiple genotypes exist (Oury et al., 2020; Schweinsberg et al., 2015). Although percent DNA methylation concordance across methods was generally high, in *P. acuta* there was approximately a 10% higher level of discordance in percent methylation quantification when compared WGBS to RRBS or MBDBS (**Figure 3**). This discordance could have resulted from differences in *P. acuta* and *M. capitata* tissue structure. There is the potential to homogenize and extract DNA from all cell types from the thin, imperforate tissues of *P. acuta*, as opposed to the thick, perforate tissues in *M. capitata* (Putnam et al., 2017), likely contributing to a greater number of cell types, and thus methylation differences, captured in our *P. acuta* samples. Furthermore, the microhabitats created in the tissues of these two species likely differ substantially spatially (Putnam et al., 2017), creating cell-to-cell variability in methylation content. Since the likelihood of capturing multiple cell types in bulk DNA extractions varies with tissue structure, future studies

should consider methods such as fluorescence-activated cell sorting (Hu et al., 2020; Rosental et al., 2017), or laser microdissection (e.g., (Liew et al., 2018)), to target specific tissues or cell types and reduce cell-to-cell methylation variability. Whereas this does not necessarily indicate a bias in our methods, it highlights the needs to account for the biological characteristics of a species when designing an experiment and evaluating results.

The gold standard for bisulfite sequencing, WGBS, can be cost prohibitive particularly if comparing multiple species and treatments. As expected, we found that WGBS performed well, particularly for *P. acuta,* which has a smaller genome. Focusing on gene orthologs, WGBS performed the best in terms of data for CpGs per gene. Based on the gene ortholog comparisons, MBDBS provided more information than RRBS for *P. acuta*, however the opposite held true for *M. capitata.* This is likely attributable to the different genome size and inherent differences in methylation that result in differential enrichment.

For both species, WGBS and MBDBS libraries covered more CpGs than RRBS libraries; however, RRBS libraries showed greater read depth for CpGs. This is because RRBS subsampled a specific, smaller portion of the genome than MBDBS or WGBS, allowing more read coverage. Hence, CpG coverage did not largely increase when deeper sequencing was modeled using RRBS data (Additional file 10: **Figure SF5**). RRBS was designed to enrich for CpG islands, short stretches of DNA with higher levels of CpGs (~1 CpG per 10bp), that are typically found in mammalian promoters and enhancer regions and thought to play a role in gene regulation (Gu et al., 2011). We found RRBS yielded a well-covered reduced representation of the genome, which is important for bisulfite data

where high read depth is desired, and locus methylation levels were concordant with WGBS for both species. However, RRBS did not enrich for promoters or other particular genomic regions compared to the other bisulfite sequencing methods (**Figure 5**), and in fact tended to identify unmethylated regions. For this reason, RRBS is not the best choice for gene-focused methylation studies in corals and other invertebrates.

A critical consideration in deciding to perform MBDBS in corals is the amount of DNA methylation present in any symbiont. If any non-target organisms have substantially more DNA methylation than the target organism, MBDBS data could become saturated by methylated DNA from non-target organisms, lowering sampling of the target species. We observed this in *P. acuta*, for which we had the genome of its Symbiodiniaceae which has ~90% genome-wide methylation (de Mendoza et al., 2018; Lohuis & Miller, 1998). When compared to RRBS and WGBS data, we found a 4 to 10-fold enrichment of Symbiodiniaceae DNA in *P. acuta* MBDBS data. Separation of host and symbionts is therefore recommended to obtain the greatest read counts for the organism of interest, but this comes at the cost of not being able to obtain RNA from the same nucleic acid pool. For example, physical separation of the host and symbiont in living cells impacts gene expression, and attempts at physical separation after freezing can degrade the host RNA. Simultaneous extraction of holobiont RNA and DNA from the same nucleic acid pool provides the optimal approach for detecting interactions between DNA methylation and epigenetic regulation of gene expression. This comes at the cost of generating excess reads to overcome highly methylated Symbiodiniaceae DNA.

MBDBS can enrich for gene regions in species where methylation is primarily found in gene bodies such as in corals (reviewed in (Eirin-Lopez & Putnam, 2019)), and can thus

provide insight into mechanisms underlying physiological or organismal responses. We found that MBDBS significantly enriched for gene bodies, specifically CDS and introns, when compared to RRBS and WGBS in both *M. capitata* and *P. acuta* (**Figure 5**). While MBDBS may be a good choice to examine gene body methylation at a reduced cost, species differences in CpG coverage within orthologous genes with MBDBS (Additional file 10: **Figure SF6**) may complicate cross-species comparisons by reducing the amount of data available for analysis. Additionally, we found high discordance between MBDBS and non-enrichment methods, WGBS and RRBS, for *P. acuta*. MBDBS is the only method we evaluated that can non-randomly sub-sample genomes present in a DNA sample through preferential pull-down of methylated DNA. Differences in methylation across the sampled genomes could result from cell-to-cell heterogeneity in methylation or cell-type (e.g., methylation of calcifying cells may differ from symbiont hosting cells). In other words, MBDBS data may represent only a subpopulation of highly methylated cells, while WGBS and RRBS represent the average methylation across all cells in the sample. Using a consistent tissue type is important to limit potential methylation heterogeneity, and caution should be taken when comparing MBDBS data directly to that of non-enrichment bisulfite sequencing approaches.

Although MBDBS did enrich for methylated regions of the genome, 80% of CpGs in *M. capitata* and 82% of CpGs in *P. acuta* interrogated with MBDBS were lowly methylated (<10% methylated) (Additional file 8: **Figure SF3**). This is expected and is consistent with previous reports applying MBDBS in other marine invertebrates where unmethylated CpGs actually represent the highest proportion of loci in the data, attributable to the nature of the methylation landscape and enrichment protocol (e.g.

(Gavery & Roberts, 2013; Venkataraman et al., 2020)). The base pair resolution of methylation revealed by MBDBS is a benefit over MBD-Seq alone because it enables a fine-scale examination of specific genomic features (e.g. exon-intron boundaries) that may not be possible with the regional resolution of MBD-Seq. Without complete knowledge of the relative importance of a single loci compared to a region, it is difficult to compare trade-offs between MBDBS and MBD-seq. However, bisulfite sequencing requires significant coverage to quantify DNA methylation.

MBDBS may have potential biases that should be considered when interpreting results. If a treatment, population comparison, or developmental change results in a given region (~500bp) going from being highly methylated to fully unmethylated, then it is likely that this region would not be interrogated by MBDBS, due to an absence of data in the unmethylated condition. This is a potential source of bias in MBDBS data and may contribute to important differentially methylated regions being overlooked: for example if one treatment results in high methylation and is captured by MBDBS and another treatment results in no methylation and is not captured by MBDBS, this region would be filtered out of the analysis because of missing data in some individuals. Further, the potential of MBDBS to provide limited information for unmethylated genes may introduce bias in studies that seek to draw relationships between methylation level and gene expression. Just as with many interpretations of key findings we present, a more complete understanding of the mechanistic functional role DNA methylation plays in genome regulation in the species of interest is needed.

There is a greater capacity to gain mechanistic insight when using methods that have single base pair resolution compared to methylation enrichment without bisulfite

615 treatment or bulk percent methylation approaches. For example, hypotheses such as the
616 linkage between DNA methylation and alternative splicing (Roberts & Gavery, 2012) are
617 more accurately tested with bisulfite sequencing approaches. We acknowledge the cost
618 of generating genomic resources and bisulfite sequencing data can be higher than other
619 approaches. While WGBS is supported here as the gold standard for DNA methylation
620 quantification, consideration should be given to specific study hypotheses in light of the
621 pros and cons of the enrichment or reduced representation approaches presented here
622 and in other comparative works (Dixon & Matz, 2020). Our results suggest that it would
623 be unwise to use multiple different library preparation methods for comparing individuals
624 within a study, especially for studies in which familial relationships are to be compared. As
625 technology advances, it would be ideal to move away from harsh bisulfite conversion to
626 assess DNA methylation with single base pair resolution across whole genomes in the
627 absence of DNA treatment (e.g., Oxford Nanopore).

628 Our results provide a quantitative comparative assessment that can be used to
629 inform the choice of sequencing DNA methylation in corals and other non-model
630 invertebrates. Together these metrics enable comparative capacity for three common
631 methods in two coral taxa that vary in their phylogeny, genome size, symbiotic unions,
632 and environmental performance, and thus provide the community with a more
633 comprehensive foundation upon which to build laboratory and statistical analyses of DNA
634 methylation, plasticity, and acclimatization.

635

636 **Abbreviations**

637 CpG: cytosine and guanine separated by a phosphate group

638 ELISA: Enzyme-Linked Immunosorbent Assay

639 MBD-seq: Methyl-CpG Binding Domain Sequencing

640 MBDBS: Methyl-CpG Binding Domain Bisulfite Sequencing

641 RRBS: Reduced representation bisulfite sequencing

642 WGBS: Whole genome bisulfite sequencing

643

644 **Acknowledgements**

645 We thank Putnam Lab members E. Strand and M. E. Schedl for their technical support.
646 Data analyses were facilitated through the use of advanced computational, storage, and
647 networking infrastructure provided by the Hyak supercomputer system at the University of
648 Washington.

649

650 **Funding**

651 This work was partially supported by the USDA: National Institute of Food and Agriculture,
652 Hatch projects RI0019-H020 to HMP, NJ01180 to DB, and the NRSP-8 National Animal
653 Genome Research Program to HMP and SBR. This work was also partially supported by
654 funding from the National Science Foundation: 1756623 to HMP, 1756616 to DB, 1921149
655 to SBR, 1921402 to JEL, and 1635423 to KEL.

656

657 **References**

658 Akalin, A., Kormaksson, M., Li, S., Garrett-Bakelman, F. E., Figueroa, M. E., Melnick, A.,
659 & Mason, C. E. (2012). methylKit: a comprehensive R package for the analysis of
660 genome-wide DNA methylation profiles. *Genome Biology*, *13*(10), R87.
661 https://doi.org/10.1186/gb-2012-13-10-r87
662 Bahr, K. D., Jokiel, P. L., & Rodgers, K. S. (2016). Relative sensitivity of five Hawaiian

coral species to high temperature under high-pCO2 conditions. *Coral Reefs* , *35*(2), 729–738. https://doi.org/10.1007/s00338-016-1405-4

Baldwin, J. M. (1902). Development and evolution, including psychophysical evolution, evolution by orthoplasy, and the theory of genetic modes. https://doi.org/10.1037/13707-000

Barshis, D. J., Ladner, J. T., Oliver, T. A., Seneca, F. O., Traylor-Knowles, N., & Palumbi, S. R. (2013). Genomic basis for coral resilience to climate change. *Proceedings of the National Academy of Sciences of the United States of America*, *110*(4), 1387–1392. https://doi.org/10.1073/pnas.1210224110

Byrne, M., Foo, S. A., Ross, P. M., & Putnam, H. M. (2020). Limitations of cross-and multigenerational plasticity for marine invertebrates faced with global climate change. *Global Change Biology*, *26*(1), 80–102. https://doi.org/10.1111/gcb.14882

Cunning, R., Ritson-Williams, R., & Gates, R. D. (2016). Patterns of bleaching and recovery of *Montipora capitata* in Kāne ʻohe Bay, Hawai ʻi, USA. *Marine Ecology Progress Series*, *551*, 131–139. https://www.int-res.com/abstracts/meps/v551/p131-139/

de Mendoza, A., Bonnet, A., Vargas-Landin, D. B., Ji, N., Li, H., Yang, F., Li, L., Hori, K., Pflueger, J., Buckberry, S., Ohta, H., Rosic, N., Lesage, P., Lin, S., & Lister, R. (2018). Recurrent acquisition of cytosine methyltransferases into eukaryotic retrotransposons. *Nature Communications*, *9*(1), 1–11. https://doi.org/10.1038/s41467-018-03724-9

Dimond, J. L., Gamblewood, S. K., & Roberts, S. B. (2017). Genetic and epigenetic insight into morphospecies in a reef coral. *Molecular Ecology*, *26*(19), 5031–5042. https://doi.org/10.1111/mec.14252

Dimond, J. L., & Roberts, S. B. (2020). Convergence of DNA Methylation Profiles of the Reef Coral *Porites astreoides* in a Novel Environment. *Frontiers in Marine Science*, *6*, 792. https://doi.org/10.3389/fmars.2019.00792

Dixon, G., Liao, Y., Bay, L. K., & Matz, M. V. (2018). Role of gene body methylation in acclimatization and adaptation in a basal metazoan. *Proceedings of the National Academy of Sciences of the United States of America*, *115*(52), 13342–13346. https://doi.org/10.1073/pnas.1813749115

Dixon, G., & Matz, M. (2020). Benchmarking DNA methylation assays in a reef-building coral. *Molecular Ecology Resources*. https://doi.org/10.1111/1755-0998.13282

Eirin-Lopez, J. M., & Putnam, H. M. (2019). Marine Environmental Epigenetics. *Annual Review of Marine Science*, *11*, 335–368. https://doi.org/10.1146/annurev-marine-010318-095114

Ewels, P., Magnusson, M., Lundin, S., & Käller, M. (2016). MultiQC: summarize analysis results for multiple tools and samples in a single report. *Bioinformatics* , *32*(19), 3047–3048. https://doi.org/10.1093/bioinformatics/btw354

Flores, K., Wolschin, F., Corneveaux, J. J., Allen, A. N., Huentelman, M. J., & Amdam, G. V. (2012). Genome-wide association between DNA methylation and alternative splicing in an invertebrate. *BMC Genomics*, *13*, 480. https://doi.org/10.1186/1471-2164-13-480

Foret, S., Kucharski, R., Pellegrini, M., Feng, S., Jacobsen, S. E., Robinson, G. E., & Maleszka, R. (2012). DNA methylation dynamics, metabolic fluxes, gene splicing,

and alternative phenotypes in honey bees. *Proceedings of the National Academy of Sciences of the United States of America*, *109*(13), 4968–4973. https://doi.org/10.1073/pnas.1202392109

Gavery, M. R., & Roberts, S. B. (2010). DNA methylation patterns provide insight into epigenetic regulation in the Pacific oyster (*Crassostrea gigas*). *BMC Genomics*, *11*(1), 483. https://doi.org/10.1186/1471-2164-11-483

Gavery, M. R., & Roberts, S. B. (2013). Predominant intragenic methylation is associated with gene expression characteristics in a bivalve mollusc. *PeerJ*, *1*, e215. https://doi.org/10.7717/peerj.215

Ghalambor, C. K., Hoke, K. L., Ruell, E. W., Fischer, E. K., Reznick, D. N., & Hughes, K. A. (2015). Non-adaptive plasticity potentiates rapid adaptive evolution of gene expression in nature. *Nature*, *525*(7569), 372–375. https://doi.org/10.1038/nature15256

Ghalambor, C. K., McKay, J. K., Carroll, S. P., & Reznick, D. N. (2007). Adaptive versus non-adaptive phenotypic plasticity and the potential for contemporary adaptation in new environments. *Functional Ecology*, *21*(3), 394–407. https://besjournals.onlinelibrary.wiley.com/doi/abs/10.1111/j.1365-2435.2007.01283.x

Gibbin, E. M., Putnam, H. M., Gates, R. D., Nitschke, M. R., & Davy, S. K. (2015). Species-specific differences in thermal tolerance may define susceptibility to intracellular acidosis in reef corals. *Marine Biology*, *162*(3), 717–723. https://doi.org/10.1007/s00227-015-2617-9

Gómez-Rubio, V. (2017). ggplot2 - Elegant Graphics for Data Analysis (2nd Edition). In *Journal of Statistical Software* (Vol. 77, Issue Book Review 2). https://doi.org/10.18637/jss.v077.b02

Gonzalez-Romero, R., Suarez-Ulloa, V., Rodriguez-Casariego, J., Garcia-Souto, D., Diaz, G., Smith, A., Pasantes, J. J., Rand, G., & Eirin-Lopez, J. M. (2017). Effects of Florida Red Tides on histone variant expression and DNA methylation in the Eastern oyster *Crassostrea virginica*. *Aquatic Toxicology* , *186*, 196–204. https://doi.org/10.1016/j.aquatox.2017.03.006

Gu, H., Smith, Z. D., Bock, C., Boyle, P., Gnirke, A., & Meissner, A. (2011). Preparation of reduced representation bisulfite sequencing libraries for genome-scale DNA methylation profiling. *Nature Protocols*, *6*(4), 468–481. https://doi.org/10.1038/nprot.2010.190

Hofmann, G. E. (2017). Ecological Epigenetics in Marine Metazoans. *Frontiers in Marine Science*, *4*, 4. https://doi.org/10.3389/fmars.2017.00004

Hu, M., Zheng, X., Fan, C.-M., & Zheng, Y. (2020). Lineage dynamics of the endosymbiotic cell type in the soft coral *Xenia*. In *Nature* (Vol. 582, Issue 7813, pp. 534–538). https://doi.org/10.1038/s41586-020-2385-7

Johnson, K. M., Sirovy, K. A., Casas, S. M., La Peyre, J. F., & Kelly, M. W. (2020). Characterizing the Epigenetic and Transcriptomic Responses to *Perkinsus marinus* Infection in the Eastern Oyster *Crassostrea virginica*. *Frontiers in Marine Science*, *7*. https://doi.org/10.3389/fmars.2020.00598

Kronholm, I., & Collins, S. (2016). Epigenetic mutations can both help and hinder adaptive evolution. *Molecular Ecology*, *25*(8), 1856–1868.

https://doi.org/10.1111/mec.13296

Krueger, F. (2012). Trim Galore: a wrapper tool around Cutadapt and FastQC to consistently apply quality and adapter trimming to FastQ files, with some extra functionality for MspI-digested RRBS-type (Reduced Representation Bisufite-Seq) libraries. *URL Http://www. Bioinformatics. Babraham. Ac. Uk/projects/trim_galore/. (Date of Access: 28/04/2016)*.

Krueger, F., & Andrews, S. R. (2011). Bismark: a flexible aligner and methylation caller for Bisulfite-Seq applications. *Bioinformatics* , *27*(11), 1571–1572. https://doi.org/10.1093/bioinformatics/btr167

Langmead, B., & Salzberg, S. L. (2012). Fast gapped-read alignment with Bowtie 2. *Nature Methods*, *9*(4), 357–359. https://doi.org/10.1038/nmeth.1923

Lewis, S. L., & Maslin, M. A. (2015). Defining the anthropocene. *Nature*, *519*(7542), 171–180. https://doi.org/10.1038/nature14258

Liew, Y. J., Howells, E. J., Wang, X., Michell, C. T., Burt, J. A., Idaghdour, Y., & Aranda, M. (2020). Intergenerational epigenetic inheritance in reef-building corals. *Nature Climate Change*, *10*(3), 254–259. https://doi.org/10.1038/s41558-019-0687-2

Liew, Y. J., Zoccola, D., Li, Y., Tambutté, E., Venn, A. A., Michell, C. T., Cui, G., Deutekom, E. S., Kaandorp, J. A., Voolstra, C. R., Forêt, S., Allemand, D., Tambutté, S., & Aranda, M. (2018). Epigenome-associated phenotypic acclimatization to ocean acidification in a reef-building coral. *Science Advances*, *4*(6), 188227. https://doi.org/10.1126/sciadv.aar8028

Liu, H., Stephens, T. G., González-Pech, R. A., Beltran, V. H., Lapeyre, B., Bongaerts, P., Cooke, I., Aranda, M., Bourne, D. G., Forêt, S., Miller, D. J., van Oppen, M. J. H., Voolstra, C. R., Ragan, M. A., & Chan, C. X. (2018). Symbiodinium genomes reveal adaptive evolution of functions related to coral-dinoflagellate symbiosis. *Communications Biology*, *1*, 95. https://doi.org/10.1038/s42003-018-0098-3

Li, Y., Liew, Y. J., Cui, G., Cziesielski, M. J., Zahran, N., Michell, C. T., Voolstra, C. R., & Aranda Lastra, M. (2018). DNA methylation regulates transcriptional homeostasis of algal endosymbiosis in the coral model *Aiptasia.  Sci Adv*, *4*.

Lohuis, M. R., & Miller, D. J. (1998). Hypermethylation at CpG-Motifs in the dinoflagellates *Amphidinium carterae* (*Dinophyceae*): Evidence from restriction analyzes, 5-azacytidine and ethionine treatment. In *Journal of Phycology* (Vol. 34, Issue 1, pp. 152–159). https://doi.org/10.1046/j.1529-8817.1998.340152.x

Meissner, A., Mikkelsen, T. S., Gu, H., Wernig, M., Hanna, J., Sivachenko, A., Zhang, X., Bernstein, B. E., Nusbaum, C., Jaffe, D. B., Gnirke, A., Jaenisch, R., & Lander, E. S. (2008). Genome-scale DNA methylation maps of pluripotent and differentiated cells. *Nature*, *454*(7205), 766–770. https://doi.org/10.1038/nature07107

Oury, N., Gélin, P., & Magalon, H. (2020). Together stronger: Intracolonial genetic variability occurrence in *Pocillopora* corals suggests potential benefits. *Ecology and Evolution*, *10*(12), 5208–5218. https://doi.org/10.1002/ece3.5807

Putnam, H. M., Barott, K. L., Ainsworth, T. D., & Gates, R. D. (2017). The Vulnerability and Resilience of Reef-Building Corals. *Current Biology: CB*, *27*(11), R528–R540. https://doi.org/10.1016/j.cub.2017.04.047

Putnam, H. M., Davidson, J. M., & Gates, R. D. (2016). Ocean acidification influences host DNA methylation and phenotypic plasticity in environmentally susceptible

corals. *Evolutionary Applications*, *9*(9), 1165–1178. https://doi.org/10.1111/eva.12408

Putnam, H. M., Roberts, S. B., & Venkataraman, Y. (2020). *Coral Methylation Methods Comparison*. Open Science Framework. https://doi.org/10.17605/OSF.IO/X5WAZ

Quinlan, A. R., & Hall, I. M. (2010). BEDTools: a flexible suite of utilities for comparing genomic features. *Bioinformatics* , *26*(6), 841–842. https://doi.org/10.1093/bioinformatics/btq033

Rice, P. M., Bleasby, A. J., & Ison, J. C. (2011). *EMBOSS User's Guide: Practical Bioinformatics with EMBOSS*. Cambridge University Press. https://play.google.com/store/books/details?id=zC5WGJxDNtcC

Riley, M., Abe, T., Arnaud, M. B., Berlyn, M. K. B., Blattner, F. R., Chaudhuri, R. R., Glasner, J. D., Horiuchi, T., Keseler, I. M., Kosuge, T., Mori, H., Perna, N. T., Plunkett, G., 3rd, Rudd, K. E., Serres, M. H., Thomas, G. H., Thomson, N. R., Wishart, D., & Wanner, B. L. (2006). *Escherichia coli* K-12: a cooperatively developed annotation snapshot--2005. *Nucleic Acids Research*, *34*(1), 1–9. https://doi.org/10.1093/nar/gkj405

Ritz, C., Baty, F., Streibig, J. C., & Gerhard, D. (2015). Dose-Response Analysis Using R. *PloS One*, *10*(12), e0146021. https://doi.org/10.1371/journal.pone.0146021

Roberts, S. B., & Gavery, M. R. (2012). Is There a Relationship between DNA Methylation and Phenotypic Plasticity in Invertebrates? *Frontiers in Physiology*, *2*, 116. https://doi.org/10.3389/fphys.2011.00116

Rodrigues, L. J., & Grottoli, A. G. (2007). Energy reserves and metabolism as indicators of coral recovery from bleaching. *Limnology and Oceanography*, *52*(5), 1874–1882. https://doi.org/10.4319/lo.2007.52.5.1874

Rodriguez-Casariego, J. A., Ladd, M. C., Shantz, A. A., Lopes, C., Cheema, M. S., Kim, B., Roberts, S. B., Fourqurean, J. W., Ausio, J., Burkepile, D. E., & Eirin-Lopez, J. M. (2018). Coral epigenetic responses to nutrient stress: Histone H2A.X phosphorylation dynamics and DNA methylation in the staghorn coral *Acropora cervicornis*. *Ecology and Evolution*, *8*(23), 12193–12207. https://doi.org/10.1002/ece3.4678

Rosental, B., Kozhekbaeva, Z., Fernhoff, N., Tsai, J. M., & Traylor-Knowles, N. (2017). Coral cell separation and isolation by fluorescence-activated cell sorting (FACS). In *BMC Cell Biology* (Vol. 18, Issue 1). https://doi.org/10.1186/s12860-017-0146-8

Schweinsberg, M., Weiss, L. C., Striewski, S., Tollrian, R., & Lampert, K. P. (2015). More than one genotype: how common is intracolonial genetic variability in scleractinian corals? *Molecular Ecology*, *24*(11), 2673–2685. https://doi.org/10.1111/mec.13200

Shumaker, A., Putnam, H. M., Qiu, H., Price, D. C., Ehud, Z., Harel, A., Wagner, N. E., Gates, R. D., Yoon, H. S., & Bhattacharya, D. (2019). Genome analysis of the rice coral *Montipora capitata*. *Scientific Reports*, *9*(2571). https://doi.org/10.1038/s41598-019-39274-3

Suarez-Ulloa, V., Rivera-Casas, C., Michel, M., & Eirin-Lopez, J. M. (2018). Seasonal variation and epigenetic changes in the flat tree oyster *Isognomon alatus* during a 2-year study of a mangrove ecosystem in North Biscayne Bay, Florida. *Journal of Shellfish Research*, 38(1):79-88 (2019). https://doi.org/10.2983/035.038.0108

Suzuki, M. M., Kerr, A. R. W., De Sousa, D., & Bird, A. (2007). CpG methylation is

targeted to transcription units in an invertebrate genome. *Genome Research*, *17*(5), 625–631. https://doi.org/10.1101/gr.6163007

Thorvaldsdóttir, H., Robinson, J. T., & Mesirov, J. P. (2013). Integrative Genomics Viewer (IGV): high-performance genomics data visualization and exploration. *Briefings in Bioinformatics*, *14*(2), 178–192. https://doi.org/10.1093/bib/bbs017

Tweedie, S., Charlton, J., Clark, V., & Bird, A. (1997). Methylation of genomes and genes at the invertebrate-vertebrate boundary. *Molecular and Cellular Biology*, *17*(3), 1469–1475. https://www.ncbi.nlm.nih.gov/pubmed/9032274

van Gurp, T. P., Wagemaker, N. C. A. M., Wouters, B., Vergeer, P., Ouborg, J. N. J., & Verhoeven, K. J. F. (2016). epiGBS: reference-free reduced representation bisulfite sequencing. *Nature Methods*, *13*(4), 322–324. https://doi.org/10.1038/nmeth.3763

Velotta, J. P., Ivy, C. M., Wolf, C. J., Scott, G. R., & Cheviron, Z. A. (2018). Maladaptive phenotypic plasticity in cardiac muscle growth is suppressed in high-altitude deer mice. *Evolution; International Journal of Organic Evolution*, *72*(12), 2712–2727. https://doi.org/10.1111/evo.13626

Venkataraman, Y. R., Downey-Wall, A. M., Ries, J., Westfield, I., White, S. J., Roberts, S. B., & Lotterhos, K. E. (2020). General DNA methylation patterns and environmentally-induced differential methylation in the eastern oyster (*Crassostrea virginica*). *Frontiers in Marine Science*. https://doi.org/10.3389/fmars.2020.00225

Vidal-Dupiol, J., Chaparro, C., Pratlong, M., Pontaroti, P., Grunau, C., & Mitta, G. (2019). Sequencing, de novo assembly and annotation of the genome of the scleractinian coral, *Pocillopora acuta*. In *bioRxiv* (p. 698688). https://doi.org/10.1101/698688

Zemach, A., McDaniel, I. E., Silva, P., & Zilberman, D. (2010). Genome-wide evolutionary analysis of eukaryotic DNA methylation. *Science*, *328*(5980), 916–919. https://doi.org/10.1126/science.1186366

## Data accessibility

The datasets supporting the conclusions of this article are available in the Coral Methylation Methods Comparison repository, http://doi.org/10.17605/OSF.IO/X5WAZ, and included included within the article (and its additional file(s)). All raw data can be accessed under NCBI Bioproject PRJNA691891.

## Author contributions

HMP designed the study and collected the samples. YRV, SAT, MRG, HMP, and SBR performed data analyses and drafted the manuscript. DB, AD-W, JME-L, KMJ, KEL, and JBP provided analytical insight and manuscript revisions. All authors read and approved the final manuscript.

## Ethics declarations

*Ethics approval and consent to participate*

The coral samples were collected under Hawai‘i Department of Aquatic Resources Special Activity Permit SAP 2019-60.

*Consent for publication*

Not applicable.

*Competing interests*

The authors declare that they have no competing interests.

## Figures and Tables

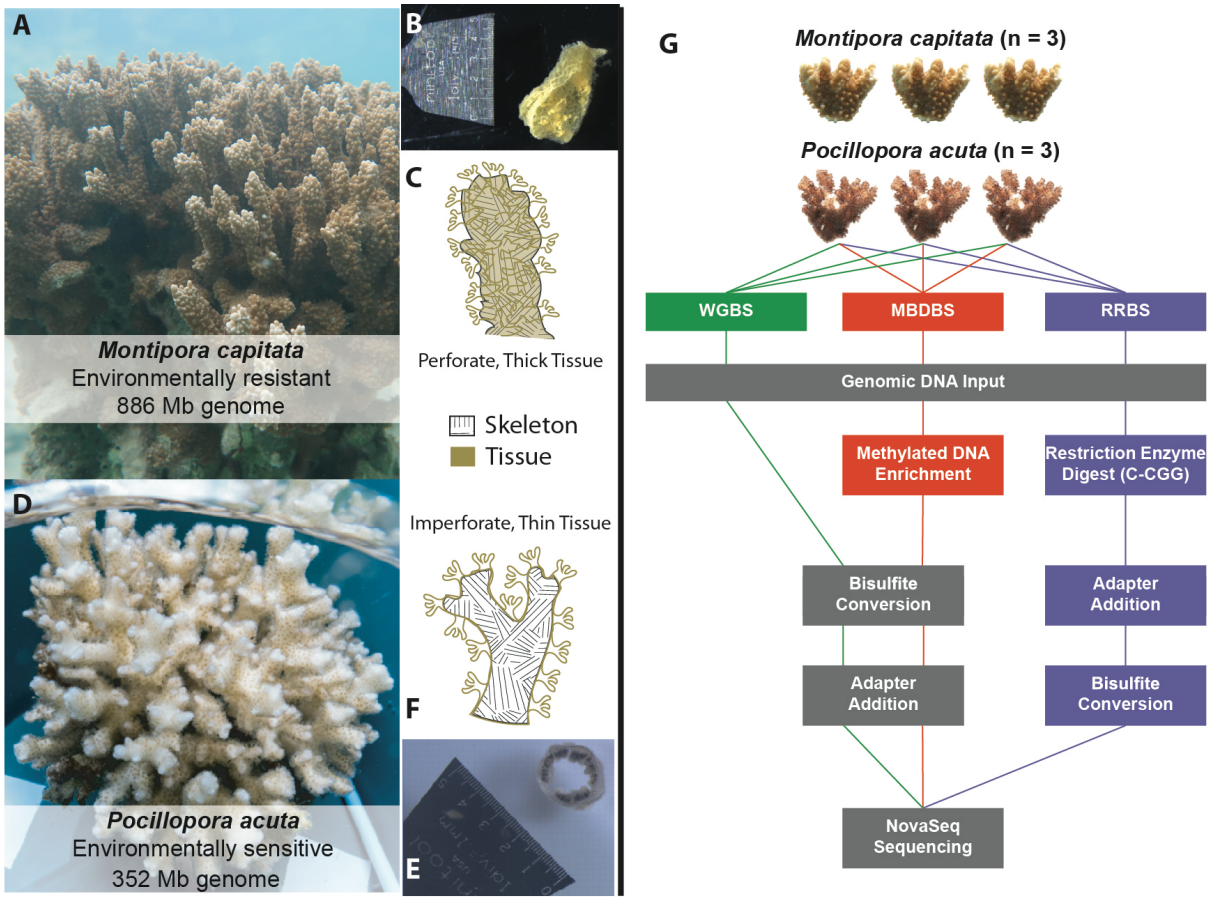


**Figure 1. Experimental design**. Three biological replicate coral samples were obtained from both coral species. A) *M. capitata*, where B) a cross section of a decalcified fragment reveals thick tissue, and C) a perforate tissue skeletal interaction. In contrast in D) *P. acuta*, a E) a cross section of a decalcified fragment reveals thin tissue, and F) an imperforate tissue skeletal interaction. DNA was extracted from each coral sample and split for use in Whole Genome Bisulfite Sequencing (WGBS), Reduced Representation Bisulfite Sequencing (RRBS), and Methyl-CpG Binding Domain Bisulfite Sequencing (MBDBS) library preparation methods. Three libraries were generated for each of the three methods, yielding nine libraries for each species and 18 libraries total.

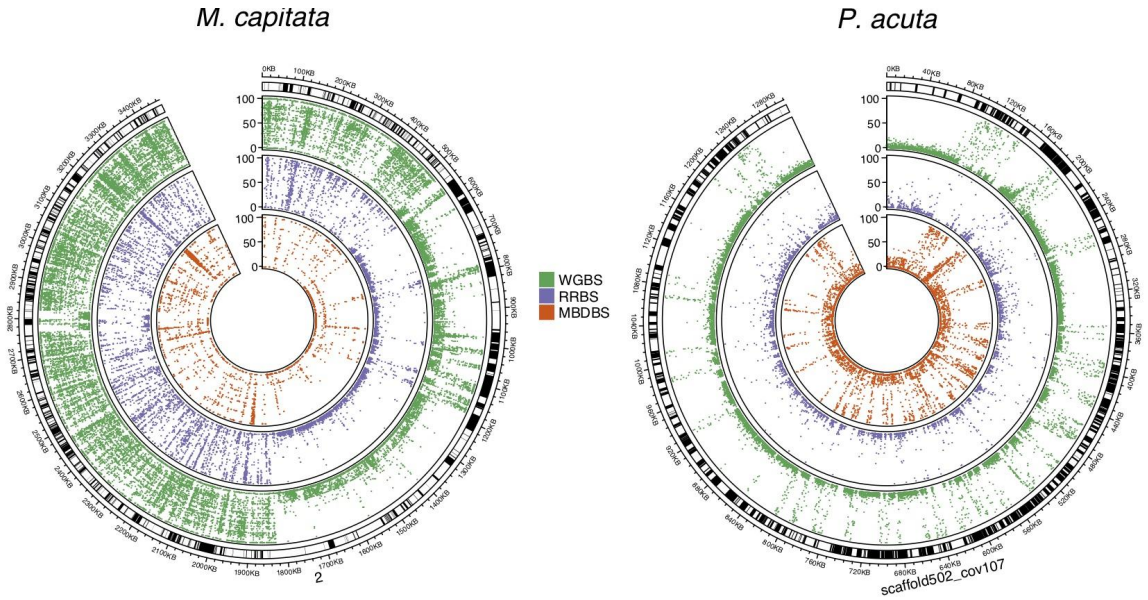


**Figure 2**. **Mean percent methylation of CpGs**. Data is presented for CpGs with 5x coverage for each method on the largest scaffolds of each genome. The outer track shows the scaffold locations and dots indicate the percent methylation as indicated by the y-axes from 0-100% for each of the inner tracks.

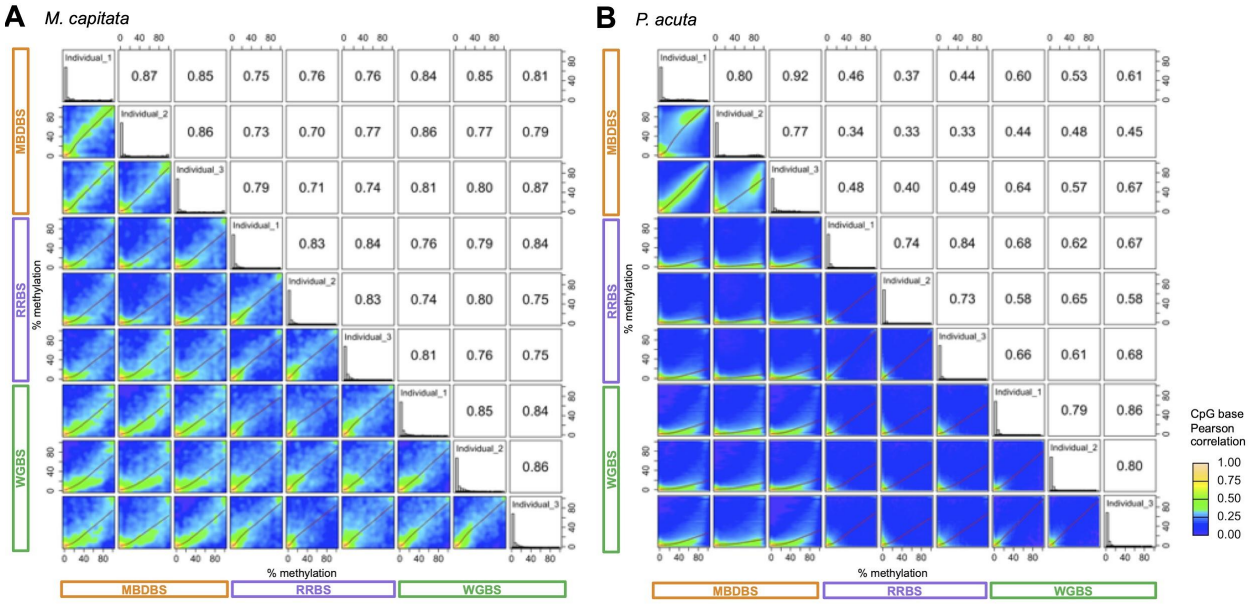


**Figure 3. Matrix of pairwise scatter plots for shared CpG loci**. Data is presented for CpG covered at ≥ 5x across all samples) for A) *M. capitata* (n=4,666 common loci) and B) *P. acuta* (n=93,714 common loci). The red lines represent linear regression fits and the

green lines are polynomial regression fits. Pearson correlation coefficients for each pairwise comparison are presented in the upper right boxes. Methods are color coded on the X and Y axes (WGBS = green, MBDBS = purple, and RRBS = orange) and replicate samples are indicated on the diagonal along with histograms of % CpG methylation.

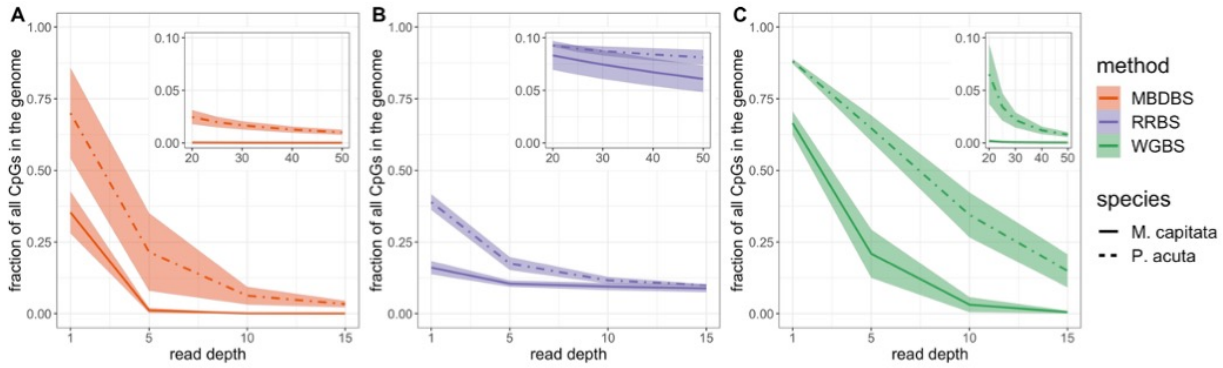


**Figure 4. CpG site coverage across library preparation methods**. Mean fraction of CpG sites in the genome covered at different sequencing depths (read depths) by (**A**) MBDBS libraries, (**B**) RRBS libraries, and (**C**) WGBS libraries with standard deviations shown by shaded areas (see Additional file 2: **Table ST2** for number of reads in each sample).

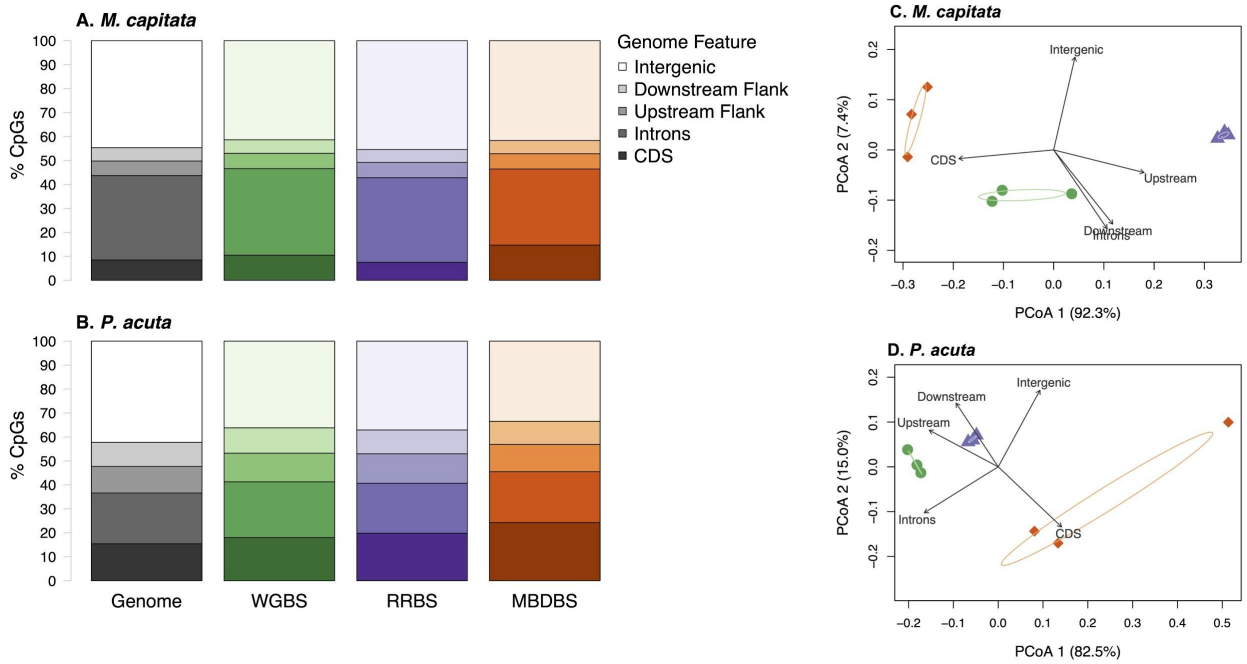


**Figure 5. Percent of CpGs detected by sequencing methods in genome features A) for *M. capitata* and B) *P. acuta*.** Genome features considered were coding sequences

(CDS), introns, 1 Kb flanking regions upstream (Upstream Flank) or downstream of genes (Downstream Flank), and intergenic regions Principal Coordinate Analyses associated with PERMANOVA and beta-dispersion tests related to Additional file 12: **Table ST6** that show differences in proportion of CpGs in various genomic locations (CDS, introns, upstream flanks, downstream flanks, and intergenic regions) for **C**) M. capitata and **D**) P. acuta. WGBS is represented by green circles, RRBS by purple triangles, and MBDBS by orange diamonds. Percent variation explained by each PCoA axis is included in the axis label. Ellipses depict 95% confidence intervals for each sequencing method. All eigenvectors are significant at the $\alpha = 0.05$ level.

## Supplementary Information